Kinetics of the NCS Radical

Randall E. Baren and John F. Hershberger*

Department of Chemistry, North Dakota State University, Fargo, North Dakota 58105

Received: August 19, 1999; In Final Form: October 20, 1999

The reaction kinetics of NCS radicals with several molecules was investigated for the first time, using laser-induced fluorescence spectroscopy to measure total rate constants and infrared absorption spectroscopy to probe possible reaction products. The NCS + NO reaction has a pressure-dependent total rate constant, with a low pressure (∼2 Torr) rate given by the expression $k_{NCS + NO} = (4.1 \pm 1.4) \times 10^{-15} \exp[(1561 \pm 116)/T]$ cm^3 $molecule^{-1}$ s^{-1} over the range 298−468 K. On the basis of the observed pressure dependence and product detection studies, this reaction is believed to be an association reaction, producing primarily NCSNO products. The NCS + NO_2 reaction was pressure-independent, with a rate constant given by $k_{NCS+NO_2} = (7.0 \pm 0.6) \times 10^{-12} \exp[(579 \pm 39.4)/T]$ cm^3 $molecule^{-1}$ s^{-1} over the range 298−620 K. No reaction of NCS with C_2H_2 or O_2 was detected, and upper limits of rate constants with these molecules were estimated at $<1.0 \times 10^{-14}$ cm^3 $molecule^{-1}$ s^{-1}.

Introduction

The kinetics of nitrogen-containing radicals in the gas phase are of great interest because of the role these species play in the formation and removal of NO_x pollutants in combustion processes.[1] For example, the NCO radical has been studied extensively, partly because it is the most important intermediate in the RAPRENO$_x$ process.[2,3] The rate constants of NCO reactions with a variety of species including NO,[4−12] NO_2,[9,10,13,14] H_2,[4,15] and several hydrocarbons[16−20] have been reported. In general, NCO reacts quickly with NO, forming $CO_2 + N_2$ and $N_2O + CO$ products in comparable yield.[12] Similarly, NCO + NO_2 is also fast, forming primarily $N_2O + CO_2$ products.[13] Hydrogen abstraction reactions of NCO with saturated hydrocarbons are generally slow,[17] with significant activation energies.[18]

The isoelectronic species NCS has been the subject of several spectroscopic studies.[21−25] The spectrum is complicated due to the presence of Renner−Teller and spin−orbit interactions. This molecule may be an intermediate in the combustion of sulfur-containing fuels. It is quite surprising, therefore, that no reports of the kinetics of this radical have previously appeared. In this study, we use laser-induced fluorescence spectroscopy to measure total rate constants of NCS with NO, NO_2, O_2, and C_2H_2. The X (000) $^2\Pi_{3/2} \rightarrow$ A (001) $^2\Pi_{3/2}$ transition at 371.41 nm[22] was chosen as the probe wavelength on the basis of strong NCS absorption and lack of interference from CN radicals. In addition, infrared absorption spectroscopy was used to search for possible reaction products.

NCS radicals were formed photolytically by two different routes. The first method used ICN or C_2N_2 precursor molecules, followed by the CN + OCS reaction:

$$ICN + h\nu\ (248\ nm) \rightarrow I + CN \qquad (1a)$$

$$C_2N_2 + h\nu\ (193\ nm) \rightarrow 2CN \qquad (1b)$$

$$CN + OCS \rightarrow NCS + CO \qquad (2)$$

Reaction 2 has been previously studied in our laboratory by infrared laser absorption spectroscopy and is quite fast, with $k_2 = 9.75 \times 10^{-11}$ cm^3 $molecule^{-1}$ s^{-1} at 298 K.[26] In some experiments, a direct NCS precursor[24] was photolyzed:

$$C_2H_5NCS + h\nu\ (193\ or\ 248\ nm) \rightarrow C_2H_5 + NCS \qquad (3)$$

Experimental Section

The photolysis laser light was provided by an excimer laser (Lambda Physik COMPEX 200) operating at 248 or 193 nm. Typical photolysis pulse energies were 2−6 mJ. The 371.41 nm probe light (∼0.1 mJ/pulse) was produced by frequency doubling 742.82 nm light from a dye laser (Continuum ND-6000) pumped by the second harmonic of an Nd:YAG laser (Lumonics J K750). The photolysis and probe beams were made collinear using a dichroic mirror and copropagated down a Pyrex reaction cell. Flourescence was detected at 90° from the laser beams using an R508 photomultiplier tube. A 400−500 nm band-pass filter was used to suppress detection of scattered laser light. The unamplified PMT signal was recorded by a boxcar integrator (Stanford Instruments model 250) with a 10 ns delay and a 300 ns gate width and averaged on a personal computer. The computer varied the delay between excimer and dye laser pulses in order to produce an NCS concentration vs time profile.

For N_2O and OCS product molecule detection, infrared absorption spectroscopy was used, as described in previous papers.[11−13] A tunable lead-salt diode laser provided the infrared probe radiation. The excimer and probe beams were made collinear with a dichroic mirror and copropagated through a 1.46 m absorption cell. The UV light was then removed with a second dichroic mirror, and the infrared light passed through a 0.25 m monochromator and was focused onto a 1 mm InSb detector (∼1 μs response). Transient infrared absorption signals were collected on a LeCroy 9310A digital oscilloscope and transferred to a computer for analysis. The HITRAN molecular infrared database[27] was used as an aid in locating N_2O absorption lines and calibrating absolute yields. OCS absorption lines were found with the aid of published spectral data.[28]

ICN (Aldrich) was purified by vacuum sublimation to remove dissolved air. OCS and SF_6 (Matheson) were purified by vacuum

---

* Corresponding author.

10.1021/jp992930e CCC: $18.00

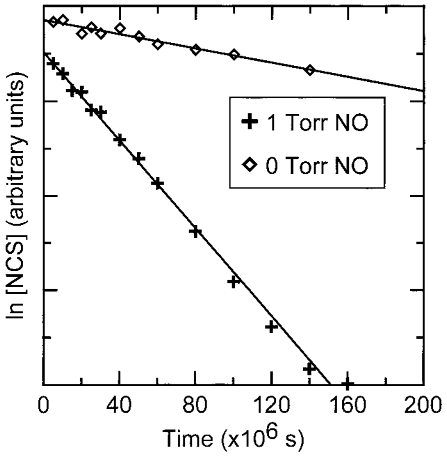

Figure 1. LIF signals of NCS as a function of time. Reaction conditions: $P_{\text{ICN}} = 0.05$ Torr; $P_{\text{OCS}} = 0.2$ Torr; $P_{\text{SF}_6} = 0.5$ Torr; $P_{\text{NO}} = 0.0$ or 1.0 Torr; $T = 296$ K. Excimer at 248 nm.

distillation at 77 K. NO_2 (Matheson) was purified by vacuum distillation at 77 and 220 K. NO (Matheson) was purified by vacuum distillation at 180 K. C_2N_2 (used in a few of the experiments) was synthesized by the reaction of copper sulfate with aqueous sodium cyanide and purified by freeze−pump−thaw cycles at 77 K.

Typical reaction conditions (using ICN precursor) were 0.05 Torr ICN, 0.5 Torr of OCS, 0.5 Torr SF_6 buffer gas, and 0.1−5.0 Torr of NO or 0.01−0.3 Torr of NO_2 reactant. On the basis of an absorption coefficient of 0.009 cm^{-1} Torr^{-1} for ICN at 248 nm,[12] typical $[\text{CN}]_0$ number densities of $\sim 4 \times 10^{12}$ were obtained. When using C_2H_5NCS precursor, ICN (or C_2N_2) and OCS were omitted and replaced by 0.05 Torr of C_2H_5NCS. Identical rate constants were measured using the different precursors.

Results

Control experiments were performed in order to verify that the LIF signals observed at 371.41 nm originate from NCS and not some other species. In particular, CN radicals have $X \rightarrow B$ transitions nearby. Photolysis of ICN/SF_6 mixtures produced no LIF signals at 371.41 nm (although strong CN signals could be observed at 388.0 nm). Only upon addition of OCS to the reaction mixture were signals observed at 371.41 nm.

NCS + NO Reaction. Figure 1 shows typical LIF signals as a function of pump−probe delay time. In the absence of added reactant, the NCS signals displayed fast rise times of a few microseconds followed by slower decay times of $\sim$100 μs. The rise is attributed to formation of NCS by reaction 2 followed by relaxation of the rovibrational energy levels to a Boltzmann distribution. Although relaxation rates for excited vibrational states of NCS are not known, the excess of SF_6 buffer gas included in each reaction mixture is expected to enhance these rates sufficiently that non-Boltzmann effects do not affect the rate constant determinations. SF_6 is known to be an efficient relaxer of vibrational excitation of several triatomic species.[29,30] The decay in the signals is attributed to removal of NCS from the reaction zone by self-reaction, reaction with other species present, or diffusion. Although some of these processes are not first order, in practice the decay portion of all of the LIF signals could be adequately fit to a single-exponential decay function, as shown in Figure 1.

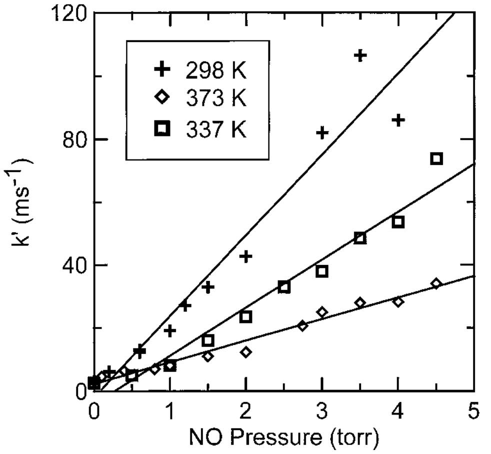

Figure 2. Pseudo-first-order decay rates of NCS LIF signals as a function of NO pressure. ICN, OCS, and SF_6 pressures are same as in Figure 1. Excimer at 248 nm.

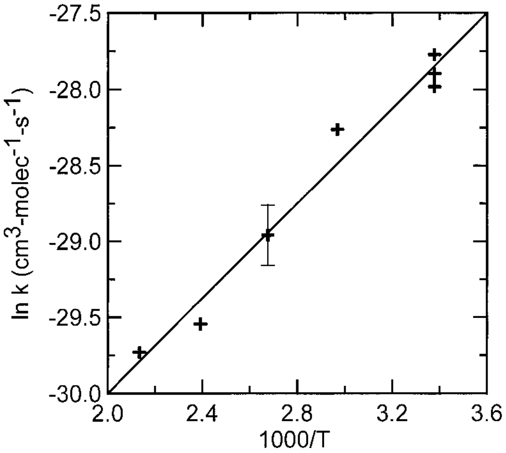

Figure 3. Arrhenius plot of the NCS + NO reaction. All data taken using ICN/OCS/NO/SF_6 mixtures as in Figures 1 and 2. Excimer at 248 nm.

When NO was included in the reaction mixture, the NCS decay rates were observed to increase. In the presence of this added reactant, pseudo-first-order conditions apply and a standard kinetic analysis shows that

$$[\text{NCS}] = [\text{NCS}]_0 \exp(-k't)$$

$$k' = k[\text{NO}] + k_{\text{D}}$$

where k' is the observed pseudo-first-order rate constant, k is the desired bimolecular rate constant for the NCS + NO reaction, and k_{D} represents the decay rate in the absence of added NO (due to other reactions, such as NCS + NCS, NCS + CN, or diffusion of NCS molecules out of the probed volume). Figure 2 shows a plot of k' vs NO pressure. From the slopes of these plots, we obtain the bimolecular rate constants.

Kinetics experiments on the NCS + NO reaction were performed over the temperature range 298−468 K. Figure 3 shows an Arrhenius plot for the measured rate constants over this range. Over the temperature range observed, no significant deviation from Arrhenius behavior was observed. The rate constants at low total pressures of $\sim$2 Torr (in cm^3 molecule^{-1} s^{-1}, 1σ error bars) are represented by

$$k_{\text{NCS + NO}} = (4.1 \pm 1.4) \times 10^{-15} \exp\,[(1561 \pm 116)/T]$$

Experiments were also performed to examine the dependence of this reaction on total pressure. Figure 4 shows the NCS + NO rate constant measured at 296 K as a function of added He.

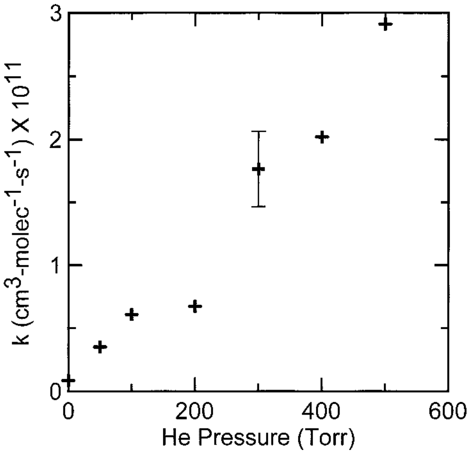

Figure 4. Dependence of NCS + NO bimolecular rate constant (at 296 K) on total pressure. Data taken using $C_2H_5NCS/NO/SF_6/He$ mixtures. Excimer at 248 nm for all points except P_{He} = 500 Torr point, for which 193 nm was used.

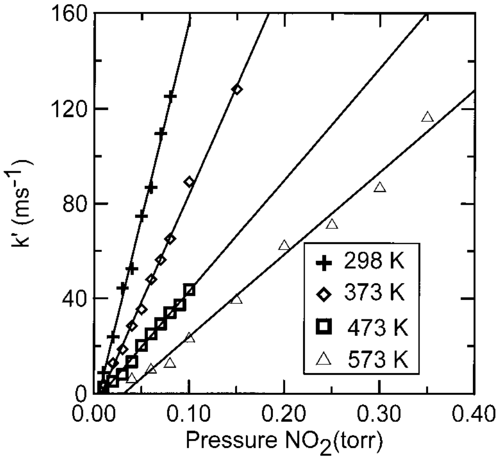

Figure 5. Pseudo-first-order decay rates of NCS LIF signals as a function of NO_2 pressure. P_{ICN} = 0.05 Torr; P_{OCS} = 1.0 Torr; P_{SF_6} = 0.5 Torr; P_{NO_2} = variable. Excimer at 248 nm.

Several possible product channels are possible for the NCS + NO reaction:

$$NCS + NO \rightarrow N_2O + CS \quad \Delta H = -32.1 \text{ kJ/mol} \tag{4a}$$

$$\rightarrow N_2 + OCS \quad \Delta H = -532.9 \text{ kJ/mol} \tag{4b}$$

$$\rightarrow NCSNO \tag{4c}$$

where thermochemical information was obtained from standard tables,[31] except for NCS, where a recent value of ΔH_f = 304.2 kJ/mol was used,[25] and for the NCSNO adduct, for which thermochemical information is unknown. Attempts to detect products in this reaction were unsuccessful. Using infrared absorption spectroscopy, no N_2O products were detected upon 248 nm photolysis of an $ICN/OCS/NO/SF_6$. No N_2O or OCS products were detected upon 193 nm photolysis of a $C_2H_5NCS/NO/SF_6$ mixture. Furthermore, no ^{18}OCS products were detected from photolysis of an $ICN/OCS/N^{18}O/SF_6$ mixture. These data suggest that channel 4c dominates this reaction. No attempt was made to detect the NCSNO adduct, for which no spectroscopic information is known.

NCS + NO₂ Reaction. When NO_2 was included in the reaction mixture, the pseudo-first-order decays rates were observed to substantially increase, as shown in Figure 5. Experiments were performed over the temperature range 298–620 K. An Arrhenius plot for the NCS + NO_2 reaction is shown in Figure 6. These data were fit to the expression (in cm^3 molecule^{-1} s^{-1})

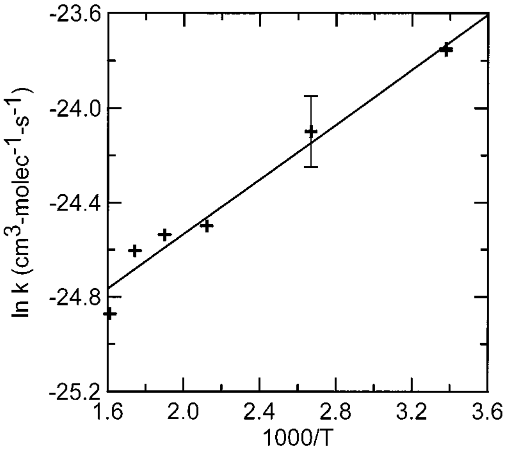

Figure 6. Arrhenius plot of the NCS + NO_2 reaction. Reaction conditions same as Figure 5. Excimer at 248 nm.

$$k_{NCS + NO_2} = (7.0 \pm 0.6) \times 10^{-12} \exp[(579 \pm 39.4)/T]$$

The dependence of this rate constant (at 296 K) on total pressure of added He was also determined and is shown in Figure 7. Within the uncertainties of the experiment, no significant pressure dependence was observed for this reaction.

Possible product channels for NCS + NO_2 include

$$NCS + NO_2 \rightarrow N_2O + OCS \quad \Delta H = -393.6 \text{ kJ/mol} \tag{5a}$$

$$\rightarrow NCSNO_2 \tag{5b}$$

$$\rightarrow CS + N_2 + O_2 \quad \Delta H = -57.0 \text{ kJ/mol} \tag{5c}$$

Using infrared absorption spectroscopy, substantial amounts of N_2O were detected upon 248 nm photolysis of an $ICN/OCS/NO_2/SF_6$ mixture. In addition to reactions 1, 2, and 5, however, we must consider secondary formation routes for N_2O, of which the most important are

$$CN + NO_2 \rightarrow NCO + NO \tag{6a}$$

$$\rightarrow N_2O + CO \tag{6b}$$

$$\rightarrow N_2 + CO_2 \tag{6c}$$

$$NCO + NO_2 \rightarrow N_2O + CO_2 \tag{7a}$$

$$\rightarrow 2NO + CO \tag{7b}$$

These reactions are fast, with k_6 = 7.2–8.9 × 10^{-11} cm^3 molecule^{-1} s^{-1} and k_7 = (0.7–2.2) × 10^{-11} cm^3 molecule^{-1} s^{-1} at 296 K.[6,32–35] Previous experiments[32,35] in our laboratory have obtained the following branching ratios for these reactions at 296 K: ϕ_{6a} = 0.87, ϕ_{6b} = 0.08, ϕ_{6c} = 0.05, ϕ_{7a} = 0.92, and ϕ_{7b} = 0.08. Thus, the primary secondary chemistry in this system is reaction 6a, which competes with reaction 2 for CN radicals. Any NCO formed in (6a) then reacts quickly with NO_2, forming significant quantities of N_2O via reaction 7a.

To test for the presence of secondary N_2O formation routes, the N_2O yields were measured as a function of OCS pressure, as shown in Figure 8. As [OCS] increases, the competition for CN radicals favors reaction 2 rather than reaction 6 so that the secondary chemistry is suppressed in the limit of high [OCS]. As shown, the N_2O product yield was observed to decay to

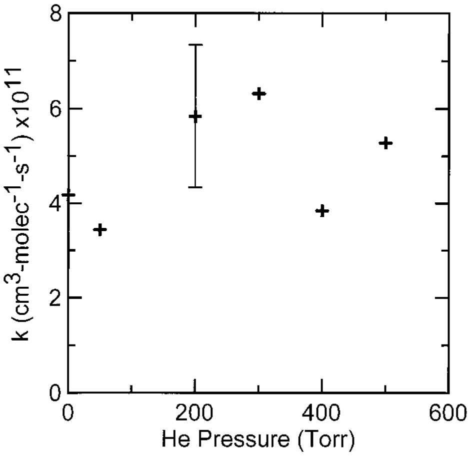

Figure 7. Dependence of NCS + NO_2 bimolecular rate constant (at 296 K) on total pressure.

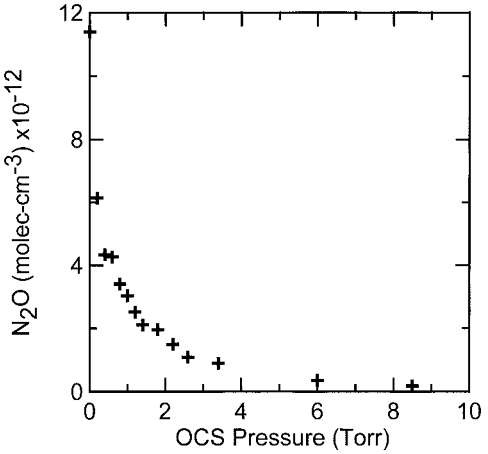

Figure 8. N_2O product yields as a function of OCS pressure. Reaction conditions: $P_{ICN} = 0.1$ Torr; $P_{SF_6} = 0.5$ Torr; $P_{NO_2} = 0.25$ Torr; P_{OCS} = variable; $T = 296$ K. Excimer at 248 nm. See text for details.

essentially zero in this limit. On the basis of these data, we conclude that virtually all of the observed N_2O products originate from then secondary reactions 6b and 7a and that the contribution of (5a) to the total NCS + NO_2 reaction is very small.

Attempts were also made to detect N_2O and OCS products upon 193 nm photolysis of a $C_2H_5NCS/NO_2/SF_6$ mixture. No OCS and only trace amounts of N_2O were detected however. This precursor also produces CN radicals in unknown yield,[36] so it is likely that the trace N_2O originated from reactions 6 and 7.

NCS + C_2H_2, O_2 Reactions. Reactions of NCS with C_2H_2 and O_2 were also investigated. No significant increase in NCS pseudo-first-order decay rates was observed upon addition of several Torr of either of these molecules however. This indicates that these reactions are extremely slow. We estimate upper limits of $<1.0 \times 10^{-14}$ cm^3 $molecule^{-1}$ s^{-1}.

Discussion

In principle, several possible secondary reactions could affect the measured rate constants. Reaction of NCS with itself or other radicals is expected to be very slow because of the low number densities used in these experiments. The pseudo-first-order rate constants in the absence of NO or NO_2 reagent were very small (<5 ms^{-1}), as shown by the near-zero intercepts in Figures 2 and 5. This suggests that radical−radical chemistry does not significantly affect the results. Other artifacts could possibly arise from reactive $O(^1D)$ or $S(^1D)$ atoms formed by 193 nm photolysis of NO_2 and OCS, respectively. Most of the reported data was taken using the 248 nm excimer wavelength, however, and our measured rate constants are independent of the excimer wavelength or NCS precursor employed.

TABLE 1: Comparison of Rate Constants (296 K) of NCO and NCS Reactions[a]

reactant	k_{NCO}	ref	k_{NCS}	ref
NO	$(3.2-3.8) \times 10^{-11}$	4−10	8.07×10^{-13}	this work
NO_2	$(0.7-2.8) \times 10^{-11}$	9, 10, 13	4.9×10^{-11}	this work
C_2H_2	1.1×10^{-13}	20	$<1.0 \times 10^{-14}$	this work
O_2	$<5.0 \times 10^{-15}$	7	$<1.0 \times 10^{-14}$	this work

[a] All rate constants in cm^3 $molecule^{-1}$ s^{-1}.

This study represents the first report of the kinetics of the NCS radical. It is worthwhile to make comparisons between the reactivity of NCS and that of the isoelectronic radical NCO, for which a significant body of literature exists. As shown in Table 1, the NCS radical is in general much less reactive than NCO at low total pressures. Unlike NCO, however, NCS reaction with NO was observed to display pressure-dependent total rate constants. This observation combined with our inability to detect reaction products from (4a) or (4b) by infrared absorption spectroscopy provides strong evidence that this reaction proceeds via stabilization of an NCSNO complex, reaction pathway 4c.

The situation with NCS + NO_2 is somewhat more uncertain. As described above, most if not all of the observed N_2O products appear to have originated from secondary chemistry, suggesting that (5a) is not a major channel. If (5b) were the major products, however, one would expect a significant dependence of k_5 on total pressure, in contrast to the experimental observations. It is possible that other product channels such as (5c) may contribute, but this channel requires substantial rearrangement on the reactive potential energy surface. Further work is necessary to resolve these issues.

Conclusion

The kinetics NCS + NO and NCS + NO_2 reactions were studied using LIF and infrared spectroscopy. Both reactions have negative temperature dependences typical of radical−radical association reactions. The NCS + NO rate constant depends on total pressure, suggesting NCSNO as the dominant product channel.

Acknowledgment. This work was supported by the Division of Chemical Sciences, Office of Basic Energy Sciences of the Department of Energy, Grant DE-FG03-96ER14645.

References and Notes

(1) Miller, J. A.; Bowman, C. T. *Prog. Energy Combust. Sci.* **1989**, *15*, 287.
(2) Perry, R. A.; Siebers, D. L. *Nature* **1986**, *324*, 657.
(3) Miller, J. A.; Bowman, C. T. *Int. J. Chem. Kinet.* **1991**, *23*, 289.
(4) Perry, R. A. *J. Chem. Phys.* **1985**, *82*, 5485.
(5) Hancock, G.; McKendrick, K. G. *Chem. Phys. Lett.* **1986**, *127*, 125.
(6) Jones, W. E.; Wang, L. *Can. J. Appl. Spectrosc.* **1993**, *38*, 32.
(7) Atakan, B.; Wolfrum, J. *Chem. Phys. Lett.* **1991**, *178*, 157.
(8) Mertens, J. D.; Dean, A. J.; Hanson, R. K.; Bowman, C. T. *Symp. (Int.) Combust. Proc.* **1992**, *24*, 701.
(9) Juang, D. Y.; Lee, J.-S.; Wang, N. S. *Int. J. Chem. Kinet.* **1995**, *27*, 1111.
(10) Wategaonkar, S.; Setser, D. W. *J. Phys. Chem.* **1993**, *97*, 10028.
(11) Cooper, W. F.; Hershberger, J. F. *J. Phys. Chem.* **1992**, *96*, 771.
(12) Cooper, W. F.; Park, J.; Hershberger, J. F. *J. Phys. Chem.* **1993**, *97*, 3283.
(13) Park, J.; Hershberger, J. F. *J. Phys. Chem.* **1993**, *97*, 13647.
(14) Wooldridge, S. T.; Mertens, J. D.; Hanson, R. K.; Bowman, C. T. *Symp. (Int.) Combust. Proc.* **1994**, *25*, 983.

(15) Louge, M. Y.; Hanson, R. K. *Combust. Flame* **1984**, *58*, 291.

(16) Perry, R. A. *Symp. (Int.) Combust. Proc.* **1986**, *25*, 913.

(17) Park, J.; Hershberger, J. F. *Chem. Phys Lett.* **1994**, *218*, 537.

(18) Schuck, A.; Volpp, H.-R.; Wolfrum, J. *Combust. Flame* **1994**, *99*, 491.

(19) Becker, K. H.; Kurtenbach, R.; Wiesen, P. *J. Phys. Chem.* **1995**, *99*, 5986.

(20) Becker, K. H.; Kurtenbach, R.; Schmidt, F.; Wiesen, P. *Chem. Phys. Lett.* **1995**, *235*, 230.

(21) Northrup, F. J.; Sears, T. J. *Chem. Phys. Lett*. **1985**, *159*, 421.

(22) Northrup, F. J.; Sears, T. J. *Mol. Phys.* **1990**, *71*, 45.

(23) Tokue, I.; Kobayashi, K.; Honda, T.; Ito, Y. *J. Phys. Chem*. **1990**, *94*, 3485.

(24) Northrup, F. J.; Sears, T. J. *J. Chem. Phys.* **1990**, *93*, 2337.

(25) Ruscic, B.; Berkowitz, J. *J. Chem. Phys.* **1994**, *101*, 7975.

(26) Park, J.; Hershberger, J. F. *Chem. Phys. Lett.* **1998**, *295*, 89.

(27) Rothman, L. S., et al. *J. Quant. Spectrosc. Radiat. Transfer* **1992**, *48*, 469.

(28) Hunt, N.; Foster, S. C.; Johns, J. W. C.; McKellar, A. R. W. *J. Mol. Spectrosc*. **1985**, *111*, 42.

(29) Fakhr, A.; Bates, R. D., Jr. *Chem. Phys. Lett*. **1980**, *71*, 381.

(30) Stephenson, J. C.; Moore, C. B. *J. Chem. Phys*. **1970**, *52*, 2333.

(31) Chase, M. W., Jr., et al. *J. Phys. Chem. Ref. Data* **1985**, *14* (suppl. 1).

(32) Park, J.; Hershberger, J. F. *J. Chem. Phys.* **1993**, *99*, 3488.

(33) You, Y. Y.; Wang, N. S. *J. Chin. Chem. Soc. (Taipai)* **1993**, *40*, 337.

(34) Wategaonkar, S.; Setser, D. W. *J. Phys. Chem*. **1993**, *97*, 10028.

(35) Park, J.; Hershberger, J. F. *J. Phys. Chem*. **1993**, *97*, 13647.

(36) Northrup, F. J.; Sears, T. J. *J. Chem. Phys.* **1990**, *93*, 2346.